

**CONFINEMENT AND PROFILE EFFECTS DURING
ICRF HEATING ON ASDEX**

K. Steinmetz, M. Brambilla, A. Eberhagen, F. Wagner, F. Wesner,
J. Bäuml, G. Becker, W. Becker, F. Braun, R. Fritsch, G. Fussmann,
O. Gehre, J. Gernhardt, G. v. Gierke, E. Glock, O. Gruber, G. Haas,
J. Hofmann, F. Hofmeister, G. Janeschitz, F. Karger, O. Klüber,
M. Kornherr, K. Lackner, G. Lisitano, F. Mast, H.-M. Mayer,
K. McCormick, D. Meisel, V. Mertens, E.R. Müller, H. Murmann,
H. Niedermeyer, J.-M. Noterdaeme, W. Poschenrieder, S. Puri, H. Rapp,
H. Röhr, J. Roth, F. Schneider, C. Setzensack, G. Siller, F. Söldner,
E. Speth, K.-H. Steuer, O. Vollmer, H. Wedler, D. Zasche

Max-Planck-Institut für Plasmaphysik,
EURATOM Association, D-8046 Garching, F.R.G.

INTRODUCTION

Various high power heating scenarios in the ion cyclotron range of frequencies (ICRF) have been studied on ASDEX up to a power of $P_{IC} \approx 2.3$ MW launched by two low-field side antennae: Hydrogen second harmonic heating ($2\Omega_{CH}$ at 67 MHz) in pure hydrogen and hydrogen-deuterium mixture plasmas, hydrogen minority heating in deuterium (D(H) at 33.5 MHz, $n_H/n_e \approx 0.05$), and the combination of both with neutral beam injection. Typical plasma data are: $R = 167$ cm, $a = 40$ cm, $I_p = 380$ kA, $B_0 \approx 2.24$ T, $\bar{n}_e = 2.6 \times 10^{13}$ cm $^{-3}$, $T_{e0} \approx 2$ keV, $T_{i0} \approx 3$ keV with double and single-null divertor configuration.

CONFINEMENT

Comparing the energy confinement of $2\Omega_{CH}$ and D(H) heating at relatively low rf power ($P_{IC} < 0.7$ MW) the D(H) minority regime exhibits no significant degradation of τ_E , which manifests itself in an enhanced ion heating efficiency and an increased direct power deposition to the electrons /1/ while the $2\Omega_{CH}$ scenario follows already an L-type scaling (Fig. 1). At higher rf power the data of both the D(H) and the $2\Omega_{CH}$ schemes can be fitted by an offset-linear scaling $W_p = W_p(0) + P_{IC} \cdot \tau_{inc}$ with incremental confinement times $\tau_{inc} = \Delta W_p^{IC} / P_{tot}$ slightly higher for D(H) ($\tau_{inc} \approx 40$ ms) than for $2\Omega_{CH}$ ($\tau_{inc} \approx 32$ ms) heating. A summary of the energy confinement with ICRH and NI in the L-mode is given in Fig. 2. A data base on ICRF H-mode confinement /2/ which could be compared with NI heating is not yet available.

PROFILE EFFECTS

During ICRH, particularly in the D(H) scheme, the electron temperature /2/ and pressure profiles are much more peaked inside the sawtooth reconnection radius ($r \approx r_{(q=1)} \sqrt{2}$) than in case of NI: this holds in particular for the combination of ICRH with NI where the energy confinement improves by about 30 % at the same total power compared to pure NI heating (Fig. 3). As far as $n_e(r)$ is concerned the electron density profiles remain essentially unchanged at the plasma boundary (between separatrix and antennae) /3/ whereas $n_e(r)$ becomes slightly

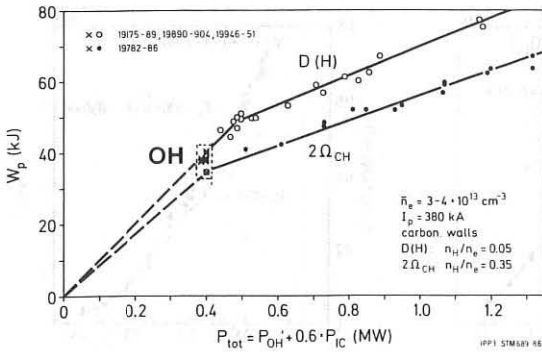


Fig. 1: Plasma energy content for $2\Omega_{CH}$ and D(H) heating versus total power (note the ICRH power absorption $\alpha = 0.6$).

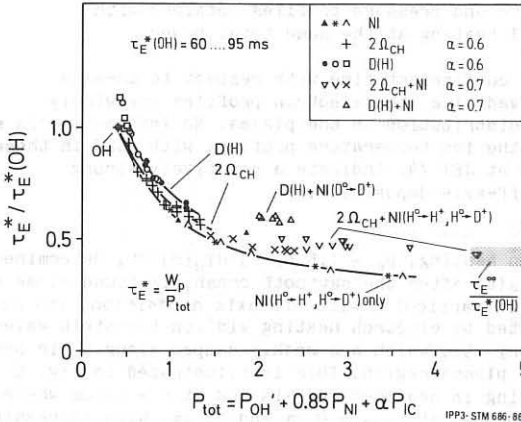


Fig. 2: Gross energy confinement times for ICRH ($2\Omega_{CH}$, D(H)), NI and ICRH+NI heating.

peaked with ICRH in the plasma centre. Whether the peakedness of the profiles and the absence or reduction of plasma rotation (in case of ICRH + NI) is directly related to the slight improvement of τ_E with ICRH is not yet clear.

The extent of temperature profile shaping has been attempted to test by varying the ICRF power deposition by either 1) shifting the $2\Omega_{CH}$ resonance layer radially while keeping $q_a = 3.3 = \text{constant}$, or 2) working with two $2\Omega_{CH}$ resonance layer positions simultaneously, excited by two antennae operating at different frequencies (67 MHz for $r_{res} = 0$ cm, and 61.9 MHz for $r_{res} \approx a/2 = 20$ cm) and variable power ($P_{IC_{tot}} = 0.9$ MW), combined with a small amount of NI heating ($P_{NI} = 0.4$ MW): In case of primarily off-axis rf power deposition neither a significant alteration of electron temperature (Fig. 4) and pressure profiles outside $q = 1$ nor a

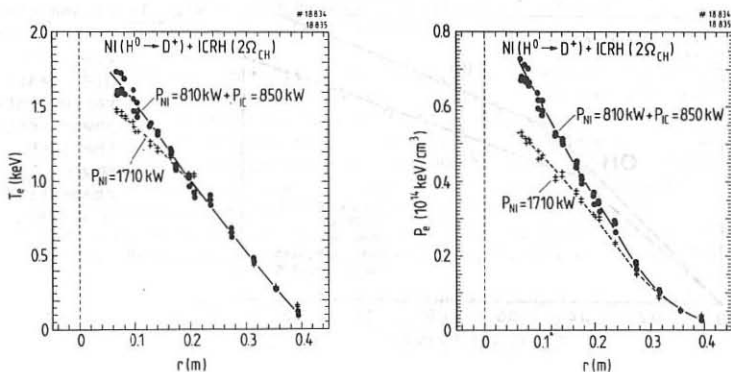


Fig. 3: Electron temperature and pressure profiles obtained with pure NI and ICRH+NI heating at the same total power.

change of the gross energy confinement time with respect to on-axis deposition have been observed, i.e. the electron profiles are widely invariant to the rf power distribution in the plasma. No information is so far available on ASDEX of the ion temperature profiles with ICRH in these conditions; investigations at JET [4] indicate a relatively strong flattening of $T_i(r)$ with off-axis deposition.

DIRECT ELECTRON HEATING

An enhanced direct electron heating, $p_e = 1.5 n_e(r) dT_e(r)/dt$, determined via the initial slope of $T_e(t)$ after the sawtooth crash, is found close to the $2\Omega_{CH}$ resonance layer, in particular with off-axis deposition. The observations can be interpreted by electron heating via ion Bernstein waves (IBW) as predicted by theory [5], which are weakly damped along their propagation towards the inner plasma region. This is illustrated in Fig. 5 where direct electron heating is measured on axis and at $r = 10$ cm whereas the resonance layers are located at $r_{res} = 0$ cm and 20 cm. With increasing ratio of off-axis to on-axis rf power direct electron heating is enhanced not only 10 cm towards the plasma centre (with respect to the off-axis resonance) but also on-axis where p_e does not decrease, although the rf power is reduced there.

SUMMARY

High power ICRF heating experiments on ASDEX and their comparison with NI heating have shown a unique confinement structure which appears to be inherent to tokamak plasmas. Although profiles are much more peaked with ICRH, their shapes are found to be invariant to modifications of the rf power deposition profiles. Studies on direct electron heating indicate that ion Bernstein waves generated via mode conversion at the $2\Omega_{CH}$ resonance layer(s) propagate more than 20 cm towards the inner plasma region while being absorbed along their path.

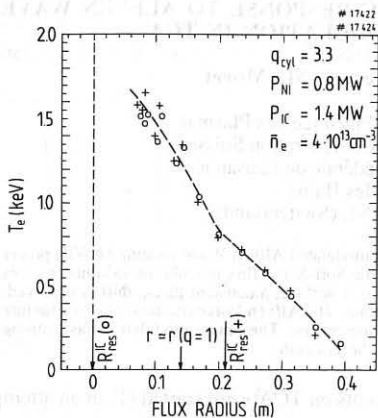


Fig. 4: Electron temperature profiles for on-axis (circles) and off-axis ICRF heating (crosses). The corresponding $2\Omega_{CH}$ resonance layers are marked by arrows.

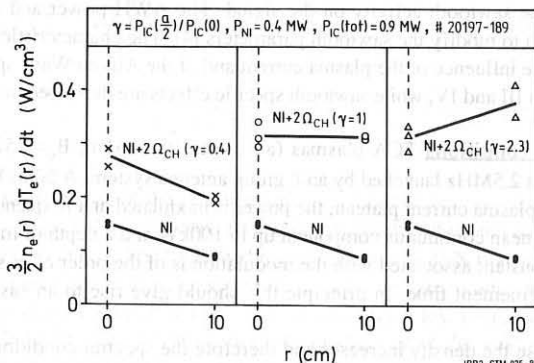


Fig. 5: Direct electron heating power density at $r = 0$ and $r = 10$ cm due to varying off-axis ICRF power deposition $\gamma = P_{IC}(a/2)/P_{IC}(0)$.

REFERENCES

- /1/ K. Steinmetz et al., Plasma Physics and Contr. Fusion **28**, 235 (1986).
- /2/ K. Steinmetz et al., 13th Europ. Conf. on Contr. Fus. and Plasma Heating, EPS Schliersee, Vol. II, 21 (1986).
- /3/ J.-M. Noterdaeme et al., this conference
- /4/ J. Jacquinet et al., RF HEATING ON JET, Proc. 11th Conf. on Plasma Phys. and Contr. Nucl. Fus. Research, Kyoto (1986).
- /5/ M. Brambilla, IPP-Report 5/15 (1987).